Fifth-Order Hyperbolic-Tangent WCNS Method Coupled with Penalization Boundary Treatment on Cartesian Grids

Qinghong Tang Yanqun Jiang*

School of Mathematics and Physics, Southwest University of Science and Technology
Mianyang, Sichuan 621010, China

* Corresponding author: jyq2005@mail.ustc.edu.cn

Supported by the Postgraduate Innovation Fund Project of Southwest University of Science and Technology (No. 26ycx2043).

1 Background and boundary treatment

Body-fitted mesh generation for complex geometries is often computationally demanding. We develop a high-resolution compressible-flow method on uniform Cartesian grids with a Brinkman penalization source term:

$$\partial_t \boldsymbol{Q} + \nabla\cdot \boldsymbol{F}_c = \nabla\cdot \boldsymbol{F}_v + \boldsymbol{S}_p,$$
$$\boldsymbol{S}_p = -\frac{\chi}{\eta_p}[0, \rho(u-u_s), \rho(v-v_s), E-E_s]^T. \tag{1}$$

Here $\phi(\boldsymbol{x})$ is the signed distance to the solid surface, with $\phi > 0$ on the fluid side. To reduce wall displacement induced by the diffuse interface, we adopt a compact-support C^1 solid indicator with transition width $\varepsilon_\chi = 0.5h$:

$$\chi(\phi) = \begin{cases} 1, & \phi \le -\varepsilon_\chi, \\ \frac{1}{2}\left[1 - \frac{\phi}{\varepsilon_\chi} - \frac{1}{\pi}\sin\left(\frac{\pi\phi}{\varepsilon_\chi}\right)\right], & |\phi| < \varepsilon_\chi, \\ 0, & \phi \ge \varepsilon_\chi. \end{cases} \tag{2}$$

The penalization term drives the conservative variables inside the solid toward their target states [5]. For a stationary cylinder, $u_s = v_s = 0$, while E_s retains local internal energy to impose an adiabatic no-slip wall. We set $\eta_p = 0.10h$.

$$\lambda_p = \frac{1-\exp(-\chi\Delta t/\eta_p)}{\Delta t}, \qquad \chi/\eta_p \;\mapsto\; \lambda_p.$$

At each RK stage, the rate above replaces χ/η_p to prevent the small relaxation scale from restricting the time step. Uniform inflow and non-reflecting outflow conditions are imposed at the outer boundaries [1,2]. Aerodynamic forces are obtained by independent surface integration of fluid-side pressure and viscous stresses. The ghost-cell result is included as an immersed-boundary reference [6].

Keywords: Cartesian grid; penalization boundary method; weighted compact nonlinear scheme; hyperbolic-tangent interpolation; compressible flow

2 Hyperbolic-tangent WCNS reconstruction

The inviscid flux uses local Lax-Friedrichs splitting and characteristic-wise reconstruction. The weighted compact nonlinear scheme (WCNS) uses the following global stencil and three substencils:

$$S = \{i-2, i-1, i, i+1, i+2\}, \quad S_k = \{i+k-2, i+k-1, i+k\},\ k = 0,1,2,$$
$$\theta = r\Delta x, \quad \mathcal{Z}_m = \tanh(m\theta)\ (m = -2,\dots,2), \quad \mathcal{Z}_{1/2} = \tanh(\theta/2).$$

The substencil interpolants, their linear combination over the global stencil, and the corresponding linear weights are given below:

$$p_k^T(x_{i+1/2}) = \sum\nolimits_{j\in S_k} f_j \prod\nolimits_{\substack{m\in S_k \\ m\ne j}} \frac{\mathcal{Z}_{1/2}-\mathcal{Z}_{m-i}}{\mathcal{Z}_{j-i}-\mathcal{Z}_{m-i}},$$
$$p_S^T(x_{i+1/2}) = \sum\nolimits_{k=0}^{2} d_k^T p_k^T(x_{i+1/2}). \tag{3}$$

$$d_0^T = \frac{(\mathcal{Z}_{1/2}-\mathcal{Z}_1)(\mathcal{Z}_{1/2}-\mathcal{Z}_2)}{2\mathcal{Z}_2(\mathcal{Z}_1+\mathcal{Z}_2)}, \qquad d_1^T = \frac{\mathcal{Z}_2^2-\mathcal{Z}_{1/2}^2}{\mathcal{Z}_2(\mathcal{Z}_1+\mathcal{Z}_2)},$$
$$d_2^T = \frac{(\mathcal{Z}_{1/2}+\mathcal{Z}_1)(\mathcal{Z}_{1/2}+\mathcal{Z}_2)}{2\mathcal{Z}_2(\mathcal{Z}_1+\mathcal{Z}_2)}. \tag{4}$$

The local smoothness indicators β_k are defined by weighted integrals of the squared first and second derivatives of each hyperbolic-tangent interpolant over target cell I_i. A second difference of the three indicators defines τ. Normalizing α_k yields the nonlinear weights ω_k:

$$\beta_k = \sum\nolimits_{\ell=1}^{2} \Delta x^{2\ell-1} \int_{I_i} [(p_k^T)^{(\ell)}]^2\,\mathrm{d}x,$$
$$\tau = \frac{(\beta_0 - 2\beta_1 + \beta_2)^2}{\sum_k \beta_k + \epsilon}, \tag{5}$$
$$\alpha_k = d_k^T\left[1 + \left(\frac{\tau}{\beta_k+\epsilon}\right)^2\right], \qquad \omega_k = \frac{\alpha_k}{\sum_l \alpha_l}.$$

At interior points, the flux derivative is evaluated as

$$(\partial_x \boldsymbol{F})_i = \frac{64}{45\Delta x}(\widehat{\boldsymbol{F}}_{i+1/2} - \widehat{\boldsymbol{F}}_{i-1/2}) - \frac{2}{9\Delta x}(\boldsymbol{F}_{i+1} - \boldsymbol{F}_{i-1}) + \frac{1}{180\Delta x}(\boldsymbol{F}_{i+2} - \boldsymbol{F}_{i-2}). \tag{6}$$

The derivative in the y direction is evaluated analogously. Sixth-order central differences discretize the viscous terms. A third-order strong-stability-preserving Runge-Kutta method advances the solution in time.

3 Numerical tests and slip-wall extension

Two-dimensional Riemann problem

The problem [3] is solved on $[0,1]^2$ using a 400×400 grid. Figure 1(a) shows that the principal shocks and contact discontinuities remain sharp. Slip-line roll-up and small-scale fluctuations are also resolved, demonstrating the shock-capturing capability of the scheme.

Flow past a circular cylinder

For cylinder flow, $\mathrm{Re} = 100$, $\mathrm{Ma}_\infty = 0.2$, $D = 1$ and $\mu = 0.01$. The $30D \times 18.75D$ computational domain is discretized by a 480×300 grid with $\Delta t = 0.00125$.

No statistics are collected for $t < 20$. After a statistically periodic state is reached, ten complete periods are sampled. Convergence of the Strouhal number St, time-averaged drag coefficient $\bar{C}_D$, and root-mean-square lift coefficient $C_{L,\mathrm{rms}}$ is verified by comparing the first five periods with the last five. The maximum relative differences are 5.81×10^{-5} for ghost-cell IBM and 1.25×10^{-5} for penalization. Here D is the characteristic length and L_r/D is the normalized recirculation length.

Mach-3 shock interaction with a cylinder

The Euler configuration follows Ref. [7]. We use 401×401 nodes and compare both methods at $t = 0.4$. The cylinder has a slip wall. IBM reflects the normal velocity, while the penalization target retains tangential velocity.

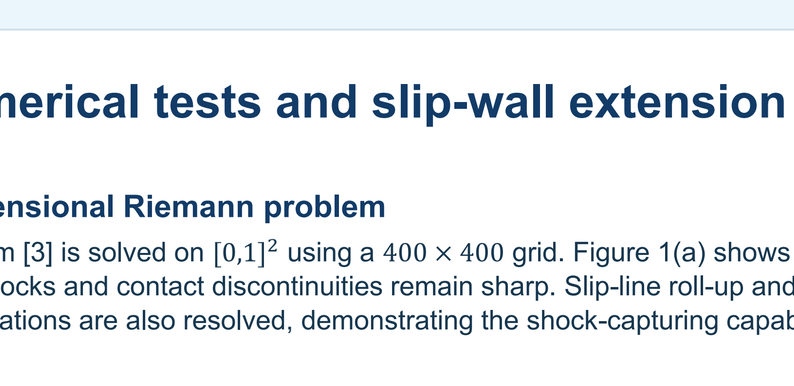


Figure 2. Density-gradient comparison at $t = 0.4$: IBM (left), penalization (right). Major reflected and diffracted shocks are similar. Near-wall differences remain in this preliminary slip-wall extension; grid/time-step convergence is not established.

4 Flow fields and quantitative results

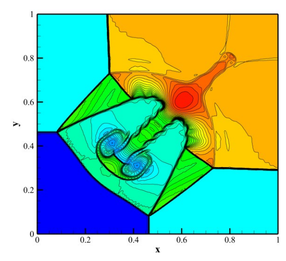


Figure 1(a). Riemann-problem density contours

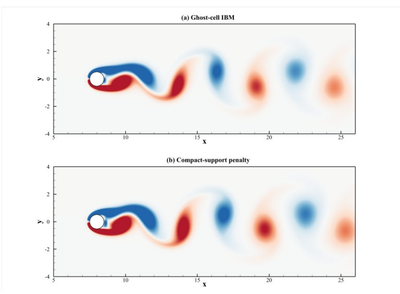


Figure 1(b). Cylinder-wake vorticity $\mathrm{Re} = 100$: IBM (top), penalization (bottom)

Both methods produce a regular Kármán vortex street in Figure 1(b). The Strouhal number obtained with the compact-support penalization method differs from the reference [4] by 0.32%. The mean drag coefficient and the magnitude of the lift fluctuations are reasonable. The flow structures and periodic statistics indicate that the method can robustly treat a non-body-fitted circular-cylinder boundary on a fixed Cartesian grid.

Table 1. Cylinder-flow statistics at $\mathrm{Re} = 100$

Method / force evaluation	$\bar{C}_D$	$C_{L,\mathrm{rms}}$	St	L_r/D
Reference [4] $\mathrm{Ma}_\infty = 0.2$	1.3190	-	0.1582	-
Ghost-cell IBM Surface integration	1.2997	0.2151	0.16697	1.2603
Compact-support penalization Independent surface integration	1.3982	0.2866	0.15870	1.1537

References

[1] Liu Q, Vasilyev OV. A Brinkman penalization method for compressible flows in complex geometries. J. Comput. Phys. 2007;227(2):946-966.
[2] Boiron O, Chiavassa G, Donat R. A high-resolution penalization method for large Mach number flows in the presence of obstacles. Comput. Fluids. 2009;38(3):703-714.
[3] Lax PD, Liu XD. Solution of two-dimensional Riemann problems of gas dynamics by positive schemes. SIAM J. Sci. Comput. 1998;19(2):319-340.
[4] Canuto D, Taira K. Two-dimensional compressible viscous flow around a circular cylinder. J. Fluid Mech. 2015;785:349-371.
[5] Angot P, Bruneau CH, Fabrie P. A penalization method to take into account obstacles in incompressible viscous flows. Numer. Math. 1999;81(4):497-520.
[6] Peskin CS. The immersed boundary method. Acta Numerica. 2002;11:479-517.
[7] Jiang Y, Yang H, Tang Q, Zhu Y. High-order WCNS scheme with a constrained weighted least squares immersed boundary method for inviscid compressible flow simulations. Adv. Aerodyn. 2026;8:9.